



Molecular Crystals and Liquid Crystals Science and Technology. Section A. Molecular Crystals and Liquid Crystals

Publication details, including instructions for authors and
subscription information:

<http://www.tandfonline.com/loi/gmcl19>

Novel Organic Ions of High-Spin States

Yoshio Teki ^a, Takeji Takui ^a, Takamasa Kinoshita ^a, Koichi Itoh ^a,
Michio Matsushita ^b, Toshihiro Nakamura ^b, Takamasa Momose ^b &
Tadamasa Shida ^b

^a Department of Chemistry, Faculty of Science, Osaka City
University, Sumiyoshi-ku, Osaka, 558

^b Department of Chemistry, Faculty of Science, Kyoto University,
Sakyo-ku, Kyoto, 606, Japan

Version of record first published: 24 Sep 2006.

To cite this article: Yoshio Teki , Takeji Takui , Takamasa Kinoshita , Koichi Itoh , Michio Matsushita ,
Toshihiro Nakamura , Takamasa Momose & Tadamasa Shida (1993): Novel Organic Ions of High-Spin
States, Molecular Crystals and Liquid Crystals Science and Technology. Section A. Molecular Crystals
and Liquid Crystals, 232:1, 271-288

To link to this article: <http://dx.doi.org/10.1080/10587259308035718>

PLEASE SCROLL DOWN FOR ARTICLE

Full terms and conditions of use: <http://www.tandfonline.com/page/terms-and-conditions>

This article may be used for research, teaching, and private study purposes. Any
substantial or systematic reproduction, redistribution, reselling, loan, sub-licensing,
systematic supply, or distribution in any form to anyone is expressly forbidden.

The publisher does not give any warranty express or implied or make any representation
that the contents will be complete or accurate or up to date. The accuracy of any
instructions, formulae, and drug doses should be independently verified with primary
sources. The publisher shall not be liable for any loss, actions, claims, proceedings,
demand, or costs or damages whatsoever or howsoever caused arising directly or
indirectly in connection with or arising out of the use of this material.

NOVEL ORGANIC IONS OF HIGH-SPIN STATES

YOSHIO TEKI, TAKEJI TAKUI, TAKAMASA KINOSHITA, KOICHI ITOH,
MICHIO MATSUSHITA*, TOSHIHIRO NAKAMURA*, TAKAMASA MOMOSE*
AND TADAMASA SHIDA*

Department of Chemistry, Faculty of Science, Osaka City University, Sumiyoshi-ku, Osaka 558, and Department of Chemistry, Faculty of Science, Kyoto University, Sakyo-ku, Kyoto 606,* Japan

Abstract The interrelation between spin alignment and a charged organic molecular field has been investigated. The monoanion (monocation) of m-phenylenbis(phenylmethylene), a ground-state quintet alternant hydrocarbon, was formed at 77 K via the photolysis of the ionized diazo precursor generated via gamma-radiolysis in the frozen solution of 2-methyltetrahydrofuran (butyl chloride). Both the ions exhibited similar ESR spectra identified as due to a ground-state quartet with $g = 2.003$ (2.003), $D = +0.1200$ (+0.1350, +0.1285) cm^{-1} and $|E| = 0.0045$ (0.0040, 0.0055) cm^{-1} for the anion (cation). The quartet state is consistent with the monoions of the parent quintet molecule with the four singly-occupied orbitals, i.e., the two π nonbonding molecular orbitals (NBMO) and the two in-plane nonbonding orbitals at the divalent carbon atoms. It was concluded by proton-ENDOR that both the excess electron and the hole occupy one of the two singly occupied π NBMO, the spins in the in-plane nonbonding orbitals being left unchanged. This was confirmed by the ESR hyperfine splitting of the divalent carbon atom labeled by C-13. In addition, the molecular conformation was found to be trans-trans for both the anion and the cation in contrast to cis-trans for the parent neutral molecule. The similar electronic structures of both the ions are consistent with the pairing theorem for the parent alternant hydrocarbon.

INTRODUCTION

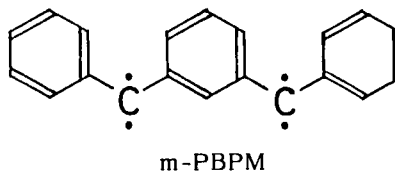
Remarkable progress has recently been made in the area of molecular-based magnetic materials, and a variety of strategies have been proposed for design and syntheses of ferromagnetic new materials. A number of these strategies have taken advantage of ionic species as constituents of such new materials as conducting magnetic materials. Understanding of the spin alignment in ionized molecular species, therefore, will be increasingly important.

It has been firmly established for neutral organic high-spin

molecules that the topology of their pi-electron networks plays an important role in intramolecular spin alignment because spins are aligned through chemical bonds. In view of the Heisenberg valence bond picture, pi-spins of an alternant hydrocarbon are aligned with alternating spin-directions on each carbon sites along its pi-electron network. As a result, we can predict the ground-state spin simply by counting the difference in number between the starred and unstarred carbon atoms of the alternant hydrocarbon,^{1,2} the difference being dependent strongly on the topology of its pi-electron network. In fact, the alternating spin distributions have been observed for a number of polycarbenes by means of ¹H-ENDOR spectroscopy, and the spin distributions observed have been shown to well interpret various features of the spin alignment of alternant polycarbenes.³⁻⁷

The nature of spin alignment described above is understood as due to the spin polarization mechanism which is known to dictate the spin alignment of neutral organic high-spin molecules. As for ionized organic high-spin molecules, however, we cannot expect such a simple guiding principle, since in ionic species we should take into account the important contribution of the spin delocalization mechanism which competes the above mechanism to yield a final spin alignment. In fact, Yamaguchi has made a predictive ab initio calculation on the possible reversal of the order of high- and low-spin states upon ionization.⁸ The interrelation between excess charge and spin alignment is interesting since this appears to be of central importance in the field not only of organic ferromagnets but also of high temperature superconductors in connection with electric conduction through copper oxide planes.^{9,10}

To develop new aspects of high spin chemistry, we have prepared ionized high-spin polycarbenes that may be potentially interesting from both an experimental and a theoretical viewpoint. As a prototype of ionized high-spin polycarbenes, a monoanion^{11,12} and a monocation¹³ of



m-phenylenebis(phenylmethylene) (m-PBPM) have been generated for the first time, and their spin states and molecular conformation has been characterized by means of ESR and ¹H-ENDOR spectroscopy. We have

chosen *m*-PBPM since it is a fundamental high-spin molecule whose optical¹⁴ as well as magnetic¹⁵ properties have been well understood.

The neutral parent molecule has four parallel spins, two of which are π spins in the two nonbonding molecular orbitals (NBMO) and are delocalized over the whole molecule, while the other two are the *n* spins in the two in-plane nonbonding orbitals "*n*" which are localized on each divalent carbon atoms. The *n* orbital is lower in energy than NBMO owing to the admixture of the 2*s* orbital, the energy gap being small since the four spins are parallel by Hund's rule. Thus, there are four singly occupied orbitals (SOMO) nearly degenerate with each other in the neutral *m*-PBPM. Hence as shown in Figure 1, the removal of one of its four electrons (spins) from the π -NBMO or the *n* orbital yields a π -cation or an *n*-cation, respectively. Similarly, the addition of an excess electron to the π -NBMO or the *n* orbital yields a π -anion or an *n*-anion, respectively. In either case, one of the four SOMO becomes a vacant or filled orbital, leading to a quartet or a doublet state as far as these four SOMO are concerned.

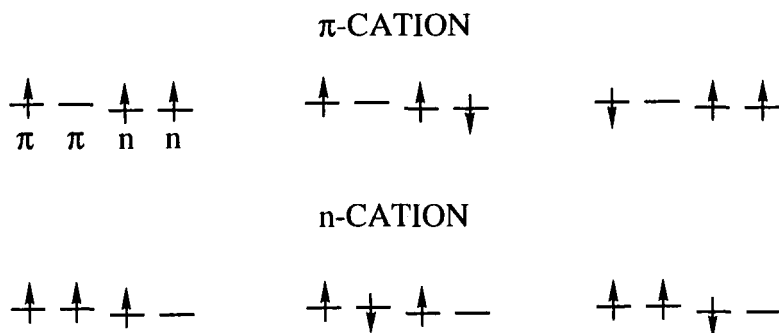


FIGURE 1 Possible spin configurations for the monocation.

This study is part of a project we have embarked on with the purpose of understanding the interrelation between spin alignment and charge in organic molecular fields. In this paper we report the novel organic ions with high-spin states with special attention to the three major problems: First, it is vital for studying magnetic properties of the ions to characterize the spin state which is either quartet or doublet, i.e., a high-spin state or a low-spin state, as shown in Figure 1. Secondly, the ionization process should be determined, since either the π or *n* SOMO takes part in the ionization processes

for both the cation and the anion formation. Thirdly, the molecular conformation is to be examined, since it may change upon ionization as a result of its energy optimization.

FORMATION OF THE MONOANION AND THE MONOCATION OF M-PBPM

The ionization was carried out by means of gamma-ray radiolysis. It has been established by Shida that gamma-ray irradiation of a frozen solution of a solute leads to a selective formation of the radical anion of the solute if we use 2-methyltetrahydrofuran (MTHF) as the solvent, whereas it leads to the radical cation of the solute if we use fureon matrix or butyl chloride (BuCl) as the solvent. In either case, an excess electron or a hole to be attached is generated by ionization of the matrix solvent.¹⁶⁻¹⁸

Then, there are two alternative methods for the formation of the target ions: Either we first generate the neutral quintet molecule via the photolysis of its diazo precursor, 1,3-bis(α -diazo-benzyl)-benzene (1,3-BDB)^{14,15} and then ionized it via radiolysis, or we first generate the ions of 1,3-BDB via radiolysis and then photolyze the ions. Unexpectedly, the first method was found to fail to generate the target ions. Thus the second method was employed.

The monoanion was formed using a MTHF solution of 1,3-BDB. The solution yielded a transparent purple glassy solid at 77 K, the color being due to the $n\pi^*$ -transition of the diazo group with $\epsilon=254$ at $\lambda_{\max}=530$ nm.¹⁴ The samples were then gamma-irradiated at 77 K to a dose of ca. 3×10^{19} eV/g. 1,3-BDB at ca. 10 mM concentration is sufficient to scavenge almost all the electrons generated by ionization of MTHF molecules. The band at 530 nm diminished upon irradiation, and an intense absorption set in at ca. 500 nm, increasing sharply toward shorter wavelengths as shown in Figure 2 (a) recorded on a Cary 14RI spectrometer. The new optical absorption is regarded as due to the radical anion of 1,3-BDB, since no optical absorption signals from solvent radicals nor from matrix-trapped electrons appear in Figure 2 (a). This inference was reinforced by a scavenge reaction of alkyl halide such as $\text{CF}_2\text{BrCF}_2\text{Br}$ suppressing the optical change drastically. Upon photobleaching with $\lambda>620$ nm at 77 K, the intense absorption appearing at $\lambda<500$ nm was replaced with new absorption bands throughout the whole range of the near-UV to near IR region, the

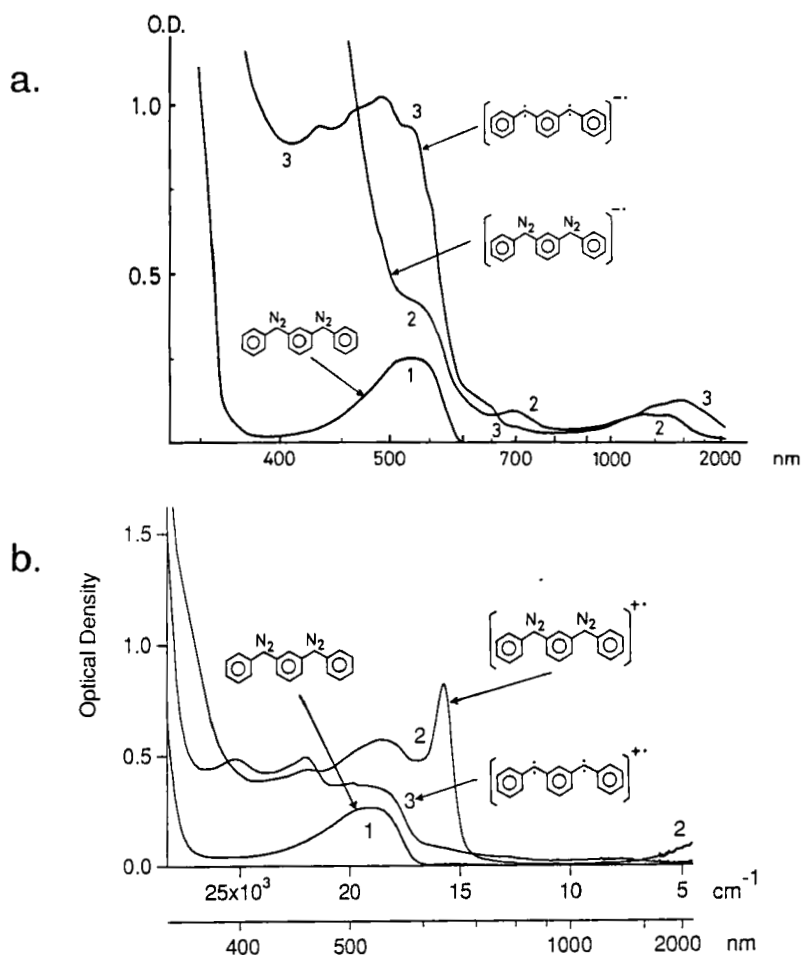
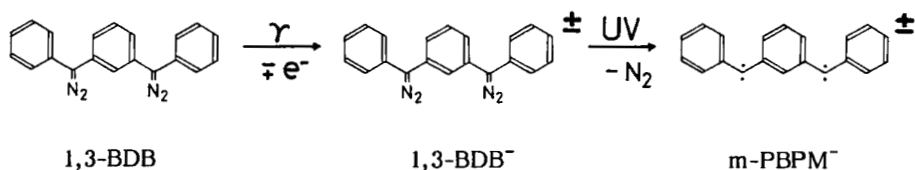


FIGURE 2 Optical absorption spectra at 77 K of (a) 1,3-BDB/MTHF solution and (b) 1,3-BDB/BuCl solution: 1, before gamma-irradiation; 2, after gamma-irradiation; 3, same as 2 but followed by photobleaching. Optical path is 1.5 mm.

major band being $\lambda_{\max}=500$ nm as shown in Figure 2 (a). This optical change can be associated with the formation of the monoanion of m-PBPM through the reaction:



as verified from the parallel change in the ESR spectrum below.

The monocation was generated using BuCl as the solvent in the manner similar to that of the monoanion. Gamma-irradiation yielded the solute cation 1,3-BDB⁺ through the charge transfer from the solvent cation BuCl⁺ produced via radiolysis, with the butyl radical and the chloride anion as the major byproducts. The optical absorption spectra at this stage is shown in Figure 2 (b). Since the byproducts are colorless in the observed region, the spectrum in curve 2 was attributed to 1,3-BDB⁺, although part of the $n\pi^*$ -transition due the intact 1,3-BDB is superposed. This absorption spectrum has a characteristic peak at 630 nm in contrast to that of 1,3-BDB⁻ with strong absorption at $\lambda < 500$ nm in curve 2 of Figure 2 (a), the difference being attributable to the different electronic structure of the anion and the cation. Upon photolysis at 77 K with $\lambda > 550$ nm, the optical spectrum changed from curve 2 to 3 as seen in Figure 2 (b). Concomitantly, the ESR spectrum exhibited a drastic change showing the formation of a high-spin species as described below. Thus, the spectrum in curve 3 was attributed to m-PBPM⁺, the target cation with a high-spin state. Interestingly, curve 3 of Figure 2 (b) resembles to curve 3 of Figure 2 (a) except that the optical density of the former spectrum is smaller by a factor of about 2.

SPIN STATES OF THE MONOANION AND THE MONOCATION OF M-PBPM

The spin states of the ions formed as above, their ionization processes, and their molecular conformations have been successfully clarified by means of ESR and ENDOR spectroscopy. ESR experiments were performed using a Bruker ESP 300 and a JEOL PE-2X spectrometer, and ¹H-ENDOR experiments using a Bruker ESP 300/350 spectrometer.

After radiolysis, the ESR spectrum exhibited strong narrow signals in the range of 0.32-0.34 T, a region characteristic of free radicals, for both the ions. This is consistent with the formation of solvent radicals and the anion and cation of 1,3-BDB all of which are spin doublet. Upon photolysis, the above ESR spectrum showed a dramatic change for both the anion and the cation: Several new ESR signals appeared over the wide range of 0-0.6 T with the concomitant change in the optical spectrum from curve 2 to 3 in Figure 2. The spectrum observed is shown at the top of Figure 3 for the anion. Nearly the

same spectrum was also observed for the cation. Such a wide spread ESR spectrum is characteristic of high-spin molecules, being direct evidence for the formation of the target ions with high-spin states.

Identification of the widely spread ESR spectrum was carried out using an ESR simulation method which we have developed for randomly oriented species of high-spin molecules.^{19,20} Analysis was based on the effective spin Hamiltonian,

$$H = g\beta\mathbf{S}\cdot\mathbf{B} + D[S_Z^2 - S(S+1)/3] + E(S_X^2 - S_Y^2) \quad (1)$$

where g is an isotropic g factor, β is the Bohr magneton, \mathbf{B} is the external magnetic field, and D and E are the fine structure parameters. All the resonance fields and transition probabilities were obtained by an exact diagonalization of the spin Hamiltonian. A total of 6,500 orientations were sampled only for one eighth of the sphere required from the symmetry of the fine structure tensor. We assumed a Gaussian line-shape function with a linewidth of 3.6 and 4.0 mT for the anion and cation, respectively.

The best fit spin Hamiltonian parameters are listed in Table I for the anion and cation; those for the neutral parent molecule¹⁵ also given for comparison. The simulated spectrum is shown in the

TABLE I Spin Hamiltonian parameters for m-PBPM and its ions.

Species		S	D/cm ⁻¹	E /cm ⁻¹	E/D
Anion	m-PBPM ⁻	3/2	+0.1200	0.0045	0.038
Cation	m-PBPM ⁺				
	Conformer I	3/2	+0.1350	0.0040	0.030
	Conformer II	3/2	+0.1285	0.0055	0.043
Neutral	m-PBPM	2	+0.07131	0.01902	0.2667

middle of Figure 3. The peaks at the stationary fields corresponding to the principal axes of the fine structure tensor are denoted by X, Y, and Z. The stationary fields due to the $\Delta M_S = \pm 2$ and ± 3 forbidden transitions marked by F and the off-axis extra line marked by A are also shown. At the bottom is depicted the angular dependence of the resonance fields in order to clarify the origin of the stationary

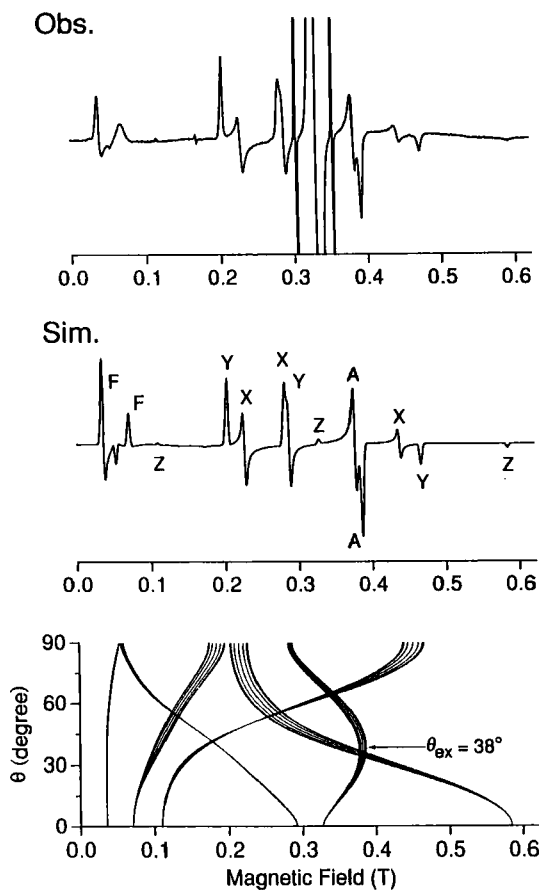


FIGURE 3 ESR spectra observed and simulated for the quartet state of $m\text{-PBPM}^-$. The angular dependence of the resonance fields is shown at the bottom. Symbols A and F denote the off-axis extra line at $\theta_{ax}=38^\circ$ and the forbidden transitions, respectively. $\nu = 9.188 \text{ GHz}$, $g = 2.003$, $D = +0.1200 \text{ cm}^{-1}$, and $|E| = 0.0045 \text{ cm}^{-1}$.

fields. The excellent agreement between the simulated and observed spectra were also attained for the cation of $m\text{-PBPM}$, which has two conformers I and II slightly different with each other in the BuCl glassy solvent. Thus, it was concluded that the ESR spectra observed are due to the quartet states of the anion and the cation of $m\text{-PBPM}$.

The off-axis extra line in powder-pattern fine-structure spectra is characteristic of high-spin states and reflects their spin multiplicities as well as their fine structure parameters.²⁰ Generally, the off-axis extra line for the $\Delta m_S = \pm 1$ allowed transitions does not occur for triplet states, but tends to appear with increasing spin multiplicities and fine structure energies and with decreasing micro-

wave frequencies. As for the half-integral spin state, however, it always occur for the transition between the central Kramers doublet ($m_S = +1/2 \leftrightarrow -1/2$). As a result, the appearance of the extra line A at $\theta = 38^\circ$ in Figure 3 strongly supports the quartet spin state.

The sign of D listed in Table I was determined to be positive from the effect of the thermal population upon the relative intensity of the ESR transitions at temperatures as low as 1.4 K. In the case of the anion, the intensity of the high-field X peak at 0.44 T was compared with that of the low-field peak at 0.22 T (see the middle of Figure 3). The high-field X peak at 9.5 K is 1.9 times as strong as that at 1.4 K. This result indicates unequivocally that the absolute sign of D is positive. The same conclusion was also derived for the cation by monitoring the Y peaks.

The quartet state observed proved to be the ground state as follows. As seen in Figure 1, the possible spin state of the ions is either quartet or doublet. Since the signal from the doublet state

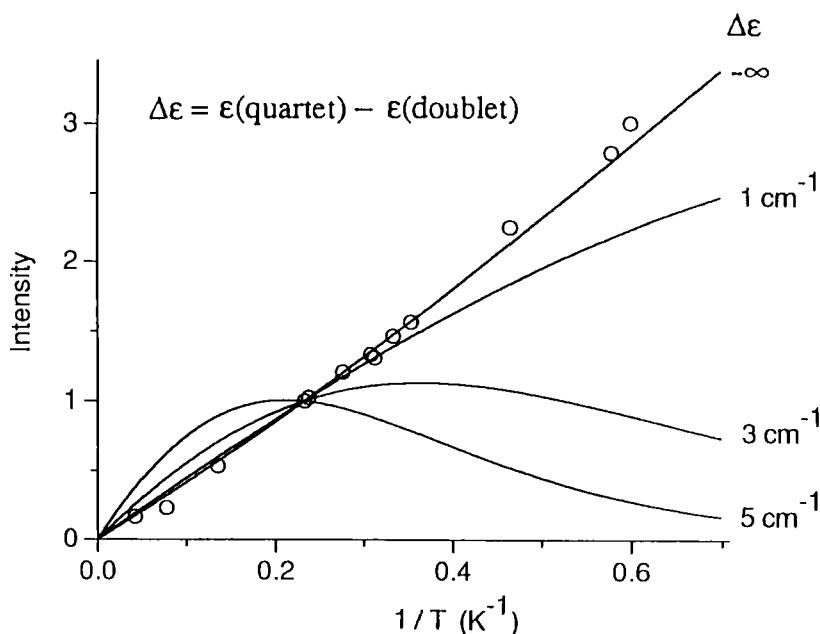


FIGURE 4 The temperature dependence of the signal intensity for the cation. The intensity of the Y peak at 200 mT is plotted as a function of reciprocal temperature.

was completely masked by the solvent radicals, we examined the Boltzmann population of the doublet state from the temperature dependence of the signal intensity of the quartet state observed. As a result of this, the ground states of both the anion and cation of m-PBPM were concluded to be quartet: Only the case of the cation is shown below. Figure 4 shows a plot of the intensity of the Y peak at 205 mT as a function of reciprocal temperature. The solid curves were calculated by considering the Boltzmann distribution in the sublevels of the quartet and the doublet states.²¹ The parameter ϵ is the energy gap of $\epsilon(\text{quartet}) - \epsilon(\text{doublet})$. The essentially linear plot fits the case of $\Delta\epsilon = -\infty$, which signifies $\epsilon(\text{quartet}) \ll \epsilon(\text{doublet})$. The possibility of $\Delta\epsilon < 1 \text{ cm}^{-1}$ can be ruled out from the absence of the quantum mixing between the nearly degenerate quartet and doublet states.

Similarly to the parent neutral molecule, both the anion and the cation have the high-spin ground state, suggesting that the spin polarization mechanism is predominant over the spin polarization mechanism in this system even in the ionized molecular field. This conclusion is supported by the ab initio calculation for m-PBPM by Yamaguchi.²² The IND0 UHF calculation shows that the quartet state is lower in energy than the doublet state for both the cation and anion in agreement with the present experiment.

Interestingly, the anion and the cation of m-PBPM exhibited quite similar ESR spectra since their ESR parameters are nearly the same as seen in Table I. This is also the same for the optical absorption spectra as shown in curve 3 of Figure 2 (a) and (b). Since m-PBPM is an alternant hydrocarbon, this resemblance between the anion and the cation is not surprising if we take the pairing theorem into account. Furthermore, this resemblance appears to justify the present characterization of the cation and the anion.

IONIZATION PROCESS AS DETERMINED BY ^1H -ENDOR

As discussed in the last part of Introduction, there are two possibilities for the cation formation by the removal of an electron, i.e., the pi-cation or the n-cation. Similarly, the pi-anion or the n-anion are expected for the anion formation by the addition of an excess electron. As for the pi-cation or the pi-anion, the spin density of the pi orbital is expected to be about one half of that of the neutral

m-PBPM, if we normalize the spin density as equal to the number of unpaired spins (see Figure 1). On the other hand, as for the n-cation and n-anion, the pi spin density will be almost unchanged since the n orbitals are nearly localized at the divalent carbon atoms.

The pi spin density on the ring carbon is proportional to the hyperfine coupling constant (hfcc) of the ring proton adjacent to that carbon atom through McConnell's equation. The hfcc's of m-PBPM and its ions are, however, too small to be observed by ESR and are hidden within the ESR linewidths. In that case, ^1H -ENDOR is a powerful tool for detecting such small hfcc's. Therefore, if we observe the ^1H -ENDOR and determine the hfcc, the pi spin density can be obtained.

To compare the hfcc of m-PBPM with that of its ions, we should take the difference in spin multiplicities into account. According to the projection theorem of angular momentum,²³ the proton hfcc is proportional to $\rho/2S$ where S denotes the total electron spin quantum number of the system studied and ρ is the spin density on the carbon adjacent to the ring proton in question. Therefore, for the pi- and the n-cation, the hfcc of the proton is expected to be 2/3 and 4/3 of that of neutral m-PBPM, respectively.

Single-crystal ENDOR provides hyperfine coupling tensors by measuring the angular dependence of the hfcc. As for a randomly oriented sample of high-spin molecules the ENDOR measurement is usually feasible only for the stationary field directions by monitoring the X, Y, and Z peaks or the off-axis extra line. Figure 5 shows the ENDOR spectra observed from the X, and the Y peak, and the extra line for the anion. These spectra were obtained by accumulation over hundreds of scans. Although the resolution is much worse than single-crystal ENDOR, this is enough to make a semi-quantitative argument.

The ENDOR frequency is given by $\nu_{\text{ENDOR}} = |\nu_n - A m_S|$ where ν_n is the Zeeman frequency of the free proton and A is the hfcc. Thus, A is simply given by the shift from the free proton frequency as divided by m_S . Therefore, if we compare the shift of the quartet ions with that of the quintet parent molecule m-PBPM, we can estimate the ratio of the pi spin density of the ions to that of the parent molecule. The maximum shift or $m_S A_{\text{max}}$ is indicated in Figure 5 for the three ENDOR spectra. The maximum shift were also observed for the cation and m-PBPM as listed in Table II. Since the hfcc is proportional to the pi

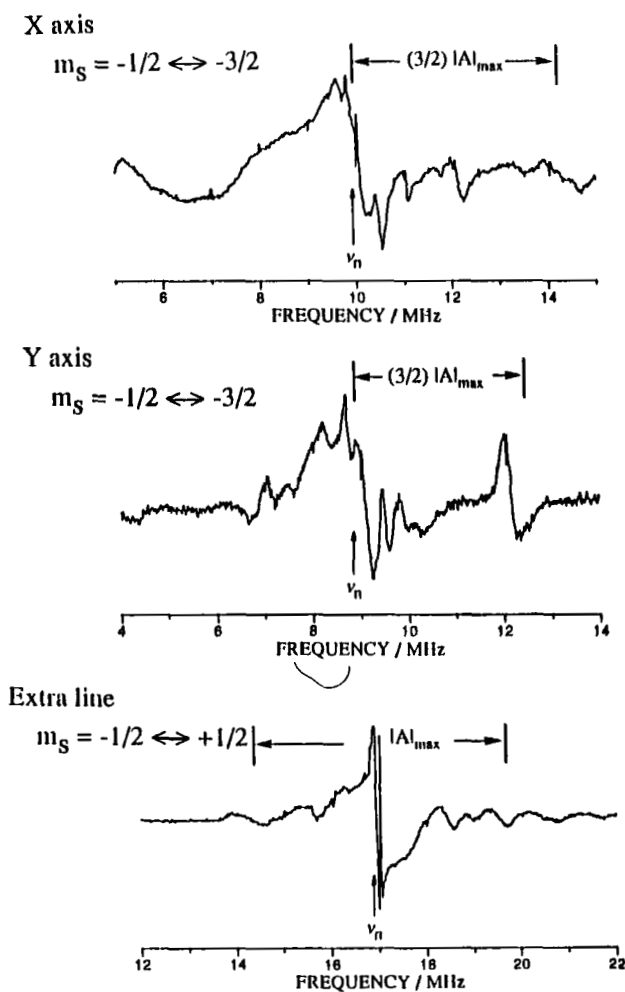


FIGURE 5 ^1H -ENDOR spectra of the anion of m-PBPM in the glassy solution of MTHF at 1.8 K. The magnetic fields are 233.3 mT (X axis), 207.8 mT (Y axis), and 397.0 mT (extra line).

spin density ρ and $1/2S$ as described before, we have

$$\begin{aligned} A_{\max}(\text{quartet})/A_{\max}(\text{quintet}) &= (4/3)[\rho(\text{quartet})/\rho(\text{quintet})] \\ &= (4/3) P_{\max} \end{aligned} \quad (2)$$

where P is the ratio of the pi spin density of the quartet state to that of the quintet state and can be estimated from A_{\max} . Table II summarizes A_{\max} and P_{\max} for m-PBPM and its anion and cation. The average ratio obtained is 0.62 for the anion and 0.57 for the cation,

TABLE II Maximum Hyperfine Coupling Constants and the ratio P_{\max} for m-PBPM and its anion and cation.

	Neutral (S=2)	A_{\max}^{Anion} /MHz (S=3/2)	Cation (S=3/2)	P_{\max}^{Anion}	P_{\max}^{Cation}
X axis	5.2	2.8	2.6	0.40	0.38
Y axis	4.8	3.5	3.3	0.55	0.51
Extra Line	5.1	5.9	5.6	0.87	0.82
Average	5.0	4.1	3.8	0.62	0.57

i.e., nearly one-half for both the ions. Since there are two pi spins in the neutral quintet molecule, these average values mean that the number of the pi spin is one for both the ions. As a result, we can safely conclude that both the excess electron and the hole occupy the pi NBMO in the process of ionization, yielding the pi-anion and the pi-cation, respectively.

IONIZATION PROCESS AS DETERMINED BY ^{13}C hfcc

The conclusion derived as above can be confirmed from the ^{13}C hfcc of ESR. When one of the two divalent carbon atoms was labeled by ^{13}C , the canonical Y and X peaks were broadened by the unresolved hfcc due to ^{13}C as shown in Figure 6. If the excess electron in the anion occupies the pi orbital, the spin density of the n orbital should remain essentially the same as that of the neutral m-PBPM, and the two divalent carbon atoms in the quartet anion will have nearly the same hfcc of 4.7 mT for H/Y axis which can be derived from the hfcc of 3.5 mT (H/Y) of the quintet m-PBPM²⁴ considering the projection factor $1/2S$. It should be noted that the Y axis is nearly parallel to the axis of the n orbital and gives the maximum ^{13}C hfcc which comes predominantly from the n spin for this direction of the magnetic field, whereas the X axis gives the minimum ^{13}C hfcc.

Since in the case of the pi-anion the spin density on both divalent carbon atoms, ^{12}C and ^{13}C , are nearly the same, the observed peak should split into a doublet due to the hfcc of the single ^{13}C . This is indicated in the left pattern at the bottom of Figure 6 where the large linewidth due to the ^1H hfcc's prevent the splittings from being

clearly resolved. On the other hand, if the excess electron resides in one of the two n orbitals, the spin density at that divalent carbon atom with a closed shell structure will be zero whether the atom is ^{12}C or ^{13}C , leading to a singlet spectrum; the spin density at the other atom will remain the same as that of the neutral m -PBPM, leading to a doublet hyperfine structure with the splitting of 4.7 mT. In the case of the n -anion, therefore, the observed hyperfine structure comprise a singlet and a doublet with equal intensity as indicated in the right pattern at the bottom of Figure 6.

The observed lineshape of the Y peak with the flat top clearly indicates that the π -anion is favored over the n -anion. This reinforces the conclusion derived from the ^1H -ENDOR experiment in the preceding chapter. On the other hand, the broadening effect due to the ^{13}C is not so clear for the X peak as for the Y peak. This is because the ^{13}C hfcc is smaller for the X peak than for the Y peak as described above. As for the cation, a quite similar ESR pattern was also observed for the Y peak at nearly 200 mT, supporting the previous conclusion that the π -cation was formed upon ionization.

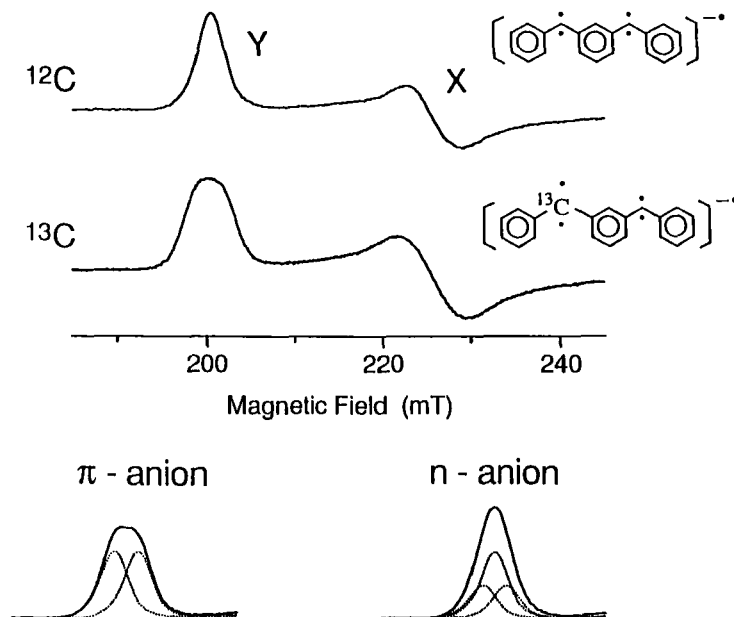


FIGURE 6 ESR Spectra of the normal and ^{13}C labeled anions of m -PBPM. Synthetic peaks for the labeled π - and n -anions are shown at the bottom.

MOLECULAR CONFORMATION OF THE ANION AND CATION OF M-PBPM

The ESR parameters obtained for m-PBPM and its anion and cation are listed in Table I, which shows that upon ionization the E/D values of both the anion and the cation remarkably change from that of neutral m-PBPM, i.e., from 0.2667 to 0.038 for the anion and to 0.030 and 0.043 for the cation. This suggests a molecular conformational change upon ionization, since the E/D value is known to be sensitive to molecular conformations. We examined this change by comparing these fine structure parameters observed with those calculated for their assumed molecular conformations using a semi-empirical method for calculating the fine structure tensor.²¹ The following description apply both the anion and the cation unless otherwise noted.

Since the spin-orbit interaction is small for aromatic hydrocarbons including polycarbenes, the dipole-dipole interaction between the electron spins is responsible for the fine structure tensor. It has been shown that the spin-spin interaction in polycarbenes arises predominantly from the one-center n-pi interaction at divalent carbon atoms.^{21,25} The fine structure tensor of aromatic polycarbenes can be represented approximately as a superposition of such interaction at each divalent carbon atoms. The fine structure tensor is, therefore, determined by both the relative orientations of the one-center interaction tensors and the spin densities at each divalent carbon atoms. Assuming that the one-center n-pi interaction can be represented by the fine structure tensor of diphenylmethylene (DPM), the ij component of the fine structure tensor for such a hydrocarbon is given by the expression²¹

$$D_{ij} = [S(2S - 1)]^{-1} \sum_k (\rho_k / \rho_{\text{DPM}}) (\mathbf{U}_k \cdot \mathbf{d}_{\text{DPM}} \cdot \mathbf{U}_k^{-1})_{ij}, \quad i, j = X, Y, Z \quad (3)$$

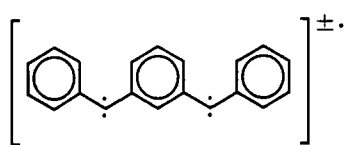
where D_{ij} stands for the ij element of the fine structure tensor of the ion, the subscript k runs over all the divalent carbon atoms and \mathbf{d}_{DPM} denotes the fine structure tensor of DPM represented in the principal axis system. The symbols ρ_k and ρ_{DPM} represent the spin density of the pi-electron at the k th divalent carbon atom of the ion and that at the divalent carbon atom of DPM, respectively. The unitary matrix \mathbf{U}_k transforms the molecule fixed axes to the principal

axes of the one-center interaction tensor at the k th divalent carbon atom. In this calculation, the bond angle of the divalent carbon atom is taken to be 150° ²⁶ and a planar structure is assumed except for the twist of the outermost phenyl groups in order to reduce the number of redundant structural parameters.

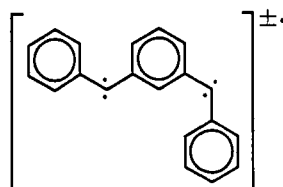
Since a simple LCAO-MO calculation gives the spin densities of $\rho_{\text{DPM}} = 2/5$ and $\rho_{\text{m-PBPM}} = 0.4040$, the ratio of these spin densities can be regarded as unity. We must take into account the projection factor $[S(2S - 1)]^{-1}$ which is 1 for the triplet DPM, 1/3 for the quartet ion, and 1/6 for the quintet m-PBPM. Since the excess electron or the hole occupies the pi orbital, the pi electron spin density will be reduced to one half of that of neutral m-PBPM. Noticing that the projection factor of the quartet ion is twice as large as that of m-PBPM together with the fact that the pi spin density reduced to one half upon ionization, we find that $D_{ij}(\text{ion})$ nearly equals $D_{ij}(\text{m-PBPM})$ if the conformation of the ion remains the same as that of m-PBPM, being in disagreement with the experiment.

TABLE III The fine structure parameters observed and those calculated for the trans-trans and trans-cis conformations.

	D/cm^{-1}	E/cm^{-1}	E/D
Observed Values			
m-PBPM ⁻	0.1200	0.0045	0.038
m-PBPM ⁺	0.1350	0.0040	0.030
	0.1285	0.0055	0.043
Calculated Values			
trans-trans	0.1292	0.0083	0.064
trans-cis	0.0819	0.0241	0.294



TRANS-TRANS



TRANS-CIS

The conformation of neutral m-PBPM is known to be trans-cis as determined by single-crystal ESR and ^1H -ENDOR spectroscopy.^{3,27} Table III compares the D , $|E|$, and $|E/D|$ values observed for the anion and cation with those calculated by the semi-empirical method described above. It can be seen that the trans-trans conformation reproduces well the observed values for both the anion and the cation, whereas the trans-cis conformation leads to a smaller D value and much larger $|E|$ and $|E/D|$ values. Thus, the molecular conformation of the anion and the cation was concluded to be trans-trans in contrast to trans-cis for the neutral parent molecule. Elucidation of the difference in the molecular structure favored by the neutral species and its ions is considered to be a crucial problem in spin chemistry. Appropriate molecular orbital calculations for ionized high-spin molecules may shed light on this problem.

CONCLUSION

Both the anion and the cation of a quintet high-spin molecule, m-PBPM, were generated in frozen solutions of MTHF and BuCl, respectively, via radiolysis and photolysis at 77 K. For both ions the ground state was determined to be quartet from the spectral simulation and from the temperature dependence of the ESR intensity. Thus, the ions as well as the parent neutral molecule have the high-spin ground state, suggesting that in such meta-linked polycarbenes the spin polarization mechanism predominates over the spin delocalization mechanism even in the negatively or positively charged molecular field. Moreover, it was found by ^1H -ENDOR and ^{13}C -ESR that both the excess electron and the hole occupy the delocalized pi NBMO upon ionization. The molecular conformations of both the anion and the cation are trans-trans in contrast to trans-cis for the neutral parent molecule. The present experiment showed that the spin alignment and the electronic structure of the cation are similar to those of the anion, being consistent with the pairing theorem for the parent alternant hydrocarbon.

ACKNOWLEDGMENT

This work was supported by Grant-in-Aid for Scientific Research on Priority Areas "Molecular Magnetism" (Area No. 228/04242103, 04242105)

from the Ministry of Education, Science and Culture, Japan.

REFERENCES

1. A. A. Ovchinnikov, Theoret. Chim. Acta, **47**, 297(1978).
2. D. J. Klein, C. J. Nelin, S. Alexander, and A. A. J. Matsen, Chem. Phys., **77**, 3101 (1982).
3. T. Takui, S. Kita, S. Ichikawa, T. Teki, T. Kinoshita, and K. Itoh, Mol. Cryst. Liq. Cryst., **176**, 67 (1989).
4. T. Takui, M. Endoh, M. Okamoto, K. Satoh, T. Shichri, Y. Teki, T. Kinoshita, and K. Itoh, Advanced Organic Solid State Materials, **173**, 63 (1990).
5. M. Okamoto, Y. Teki, T. Takui, T. Kinoshita, and K. Itoh, Chem. Phys. Letters, **173**, 265 (1990).
6. Y. Teki, K. Sato, M. Okamoto, A. Yamashita, Y. Yamaguchi, T. Takui, T. Kinoshita, and K. Itoh, Bull. Magn. Reson., (1992), in press.
7. K. Sato, Y. Yamaguchi, Y. Teki, T. Takui, T. Kinoshita, and K. Itoh, Bull. Magn. Reson., to be published.
8. K. Yamaguchi, Y. Toyoda, T. Fueno, Synth. Met., **19**, 81 (1987).
9. G. Gaskaran, Z. Zou, and P. W. Anderson, Solid State Commun., **63**, 973 (1987).
10. P. W. Anderson, G. Baskaran, Z. Zou, and T. Hsu, Phys. Rev. Letters, **58**, 2790 (1987).
11. M. Matsushita, T. Momose, T. Shida, Y. Teki, T. Takui, and K. Itoh, J. Am. Chem. Soc., **112**, 4700 (1990).
12. M. Matsushita, T. Nakamura, T. Momose, T. Shida, Y. Teki, T. Takui, T. Kinoshita, and K. Itoh, J. Am. Chem. Soc., **114**, 7470 (1992).
13. M. Matsushita, T. Nakamura, T. Momose, T. Shida, Y. Teki, T. Takui, T. Kinoshita, and K. Itoh, Bull. Chem. Soc. Jpn., (1993), in press.
14. K. Itoh, H. Konishi, N. Mataga, J. Chem. Phys., **48**, 4789 (1968).
15. K. Itoh, Chem. Phys. Letters, **1**, 235 (1967).
16. T. Shida, E. Haselbach, and T. Bally, Acc. Chem. Res., **17**, 180 (1984).
17. T. Shida, Electronic Absorption Spectra of Radical Ions. Physical Science Data **34**, (Elsevier Science Publishers, Amsterdam, 1988), p. 446.
18. T. Shida, Annu. Rev. Phys. Chem., **42**, 55 (1991).
19. Y. Teki, T. Takui, H. Yagi, K. Itoh, and H. Iwamura, J. Chem. Phys., **83**, 539 (1985).
20. Y. Teki, T. Takui, and K. Itoh, J. Chem. Phys., **88**, 6134 (1988).
21. Y. Teki, T. Takui, K. Itoh, H. Iwamura, and K. Kobayashi, J. Am. Chem. Soc., **108**, 2147 (1986).
22. M. Okumura, K. Takada, J. Maki, T. Noro, W. Mori, and K. Yamaguchi, Mol. Cryst. Liq. Cryst., Proceedings of this Symposium.
23. M. E. Rose, Elementary Theory of Angular Momentum (John Wiley & Sons, New York, 1957).
24. Y. Teki, T. Takui, and K. Itoh, unpublished.
25. J. Higuchi, J. Chem. Phys., **38**, 1237 (1963); **39**, 1847 (1963).
26. J. Higuchi, Bull. Chem. Soc. Jpn., **43**, 3773 (1970).
27. K. Itoh, Pure Appl. Chem., **50**, 1251 (1978).